Theoretical Study of Damage to DNA by 0.2−1.5 eV Electrons Attached to Cytosine†

Joanna Berdys,‡,§ Iwona Anusiewicz,‡,§ Piotr Skurski,‡,§ and Jack Simons*,‡

Chemistry Department and Henry Eyring Center for Theoretical Chemistry, University of Utah, Salt Lake City, Utah 84112 and Department of Chemistry, University of Gdansk, 80-952 Gdansk, Poland

Received: July 7, 2003

We extended our earlier study on single strand break (SSB) formation in DNA induced by low-energy electrons that attach to DNA bases' π^*-orbitals. In particular, we examined a range of electron energies (E) representative of the Heisenberg width of the lowest π^*-resonance state of cytosine, and we considered how the SSB rates depend on E and on the solvation environment. Moreover, we evaluated the adiabatic through-bond electron transfer rate with which the attached electron moves from the base, through the deoxyribose, and onto the phosphate unit. Our findings show that the SSB rate depends significantly on the electron energy E and upon the solvation environment near the DNA base. For example, in solvation characterized by a dielectric constant of 4.9, the rates range from 10^0 to 10^7 s^{-1} as the electrons' kinetic energy varies from 0.2 to 1.5 eV. We also find that the rate of through-bond electron transfer is not the factor that limits SSB formation; rather, it is the rate at which a barrier is surmounted on the anion's energy surface and it is this barrier that depends on E and on solvation.

I. Introduction

There are many ways by which DNA can be damaged, but in this work we focus only on the effects of free (i.e., nonsolvated) electrons in inducing lesions because recent experimental results[1] have shown that even very low energy electrons may be implicated, although the mechanism by which such damage occurs still needs to be elucidated. It is this mechanistic goal that forms the primary emphasis of this work, which is an extension of our earlier study.[2] A broader perspective about DNA damage can be found in several review sources[3] that overview the other myriad of chemical, radiative, and electron-initiated mechanisms by which DNA suffers damage.

In our earlier effort, we reported[2] results of a theoretical simulation that suggested the mechanism for DNA damage that may be operative in the experiments of ref 1. Specifically, we suggested that DNA undergoes C−O bond cleavage at the bond connecting the deoxyribose and phosphate units via a mechanism in which a low-energy electron enters a π^*-orbital of one of DNA's bases, after which the electron migrates through the adjoining deoxyribose unit and into the σ^*-orbital of the C−O bond mentioned above, at which time a single strand break (SSB) occurs producing a carbon radical and a phosphate group anion.

By no means is this mechanism suggested to be dominant or even operative in all cases, but it is likely to be involved in the experiments detailed in ref 1. These experiments[1] were preformed on DNA samples that had been deposited onto a tantalum substrate and subjected to vacuum desiccation that removed all but ca. 2.5 water molecules per base pair (i.e., the so-called structural water). As a result, these rather dry samples no doubt had countercations closely bound to the DNA's phosphate groups, thus rendering these groups charge neutral and thus not repulsive to an added electron. Such samples are probably best described as having solvation environments more appropriate to a gas-phase sample than to in vivo DNA. Certainly, both the experimental findings and our theoretical study related to such samples of DNA must not be used to draw more general conclusions about DNA in other environments. However, we believe that the results obtained on such DNA can offer insight into what can happen in living organisms under very specific circumstances that we detail later.

The model system treated in ref 2 consisted of the cytosine-containing fragment shown in Figure 1 but with the negative charge in each phosphate group terminated by protonation, which we used to simulate the presence of the tightly associated countercations that certainly are present in the samples of ref 1. That is, the system has no net charge prior to attaching a single excess electron and the phosphate groups are neutral.

After placing an electron into the lowest unoccupied molecular orbital (LUMO) of the cytosine unit,[4] we examined the energy landscape of the resulting π^*-anion and found that the C−O bond labeled above was much more susceptible to cleavage than it was in the absence of the attached electron. That is, homolytic cleavage of this C−O bond in the absence of the attached electron requires ca. 100 kcal mol^{-1}. In contrast, for the anion, rupture of this same C−O bond required surmounting only a 13 kcal mol^{-1} barrier. The origin of this extremely large change in the energy needed to break the C−O bond lies in the very large (ca. 5 eV) electron affinity of the neutralized phosphate group $(RO)_2OP-O$ that is formed as the C−O bond breaks. Therefore, we suggested that, although the incident electron initially attaches to a base π^*-orbital, it eventually makes its way, through the intervening deoxyribose, onto the oxygen atom of the phosphate group formed when the C−O bond breaks. The migration of the electron is illustrated in Figure 2. Of course, this process also creates a carbon radical center on the deoxyribose, and this radical can subsequently induce further damage in neighboring regions of the DNA.

One might wonder why the incident electrons cannot attach directly to the C−O bond (more correctly, be captured into the σ^*-orbital of this bond) and thus cause this bond to break in a

† Part of the special issue "Fritz Schaefer Festschrift".

* Corresponding author. E-mail: simons@chemistry.utah.edu.
‡ University of Utah.
§ University of Gdansk.

10.1021/jp035957d CCC: $27.50
Published on Web 11/21/2003

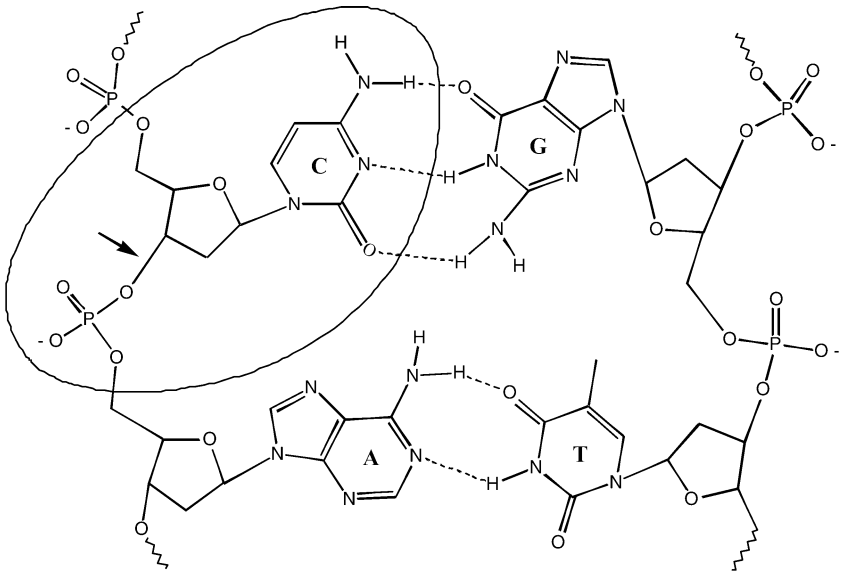

Figure 1. Excised fragment of DNA containing cytosine (circled) showing the C−O bond that ruptured (arrow) in the simulations of ref 2.

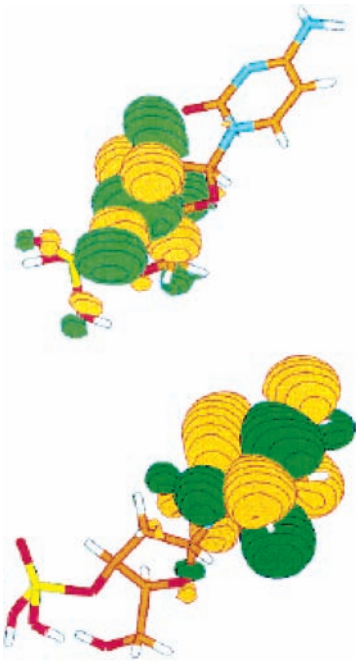

Figure 2. Orbital occupied by the attached electron on the cytosine (bottom) and for elongated C−O bond lengths (top) where the electron has migrated to the phosphate group.

more direct manner. Certainly, such dissociative electron attachment processes are known to occur. The problem with this suggestion lies in the fact that, near the equilibrium C−O bond length, the C−O σ^*-orbital lies too high in energy to be accessed by the very low energy electrons we studied. At higher electron kinetic energies, direct dissociative electron attachment may be involved, but probably not in the experiments of ref 1 and certainly not in our simulations. However, as we detail later, this σ^*-orbital does come into play in the mechanism proposed in ref 2 once the C−O bond becomes elongated (e.g., due to thermal vibrations). In particular, once this bond is stretched sufficiently, the energy of the σ^*-anion decreases and allows the attached electron to flow from the cytosine π^*-orbital, onto the C−O σ^*-orbital, and eventually into the very attractive phosphate group.

Let us now return to our discussion of what our earlier study concluded. Using the ca. 13 kcal mol^{-1} barrier to C−O bond cleavage on the anion surface mentioned above and estimating the frequency at which the C−O bond vibrates to be 3×10^{13} s^{-1}, we predicted the rate for passage over the barrier to be ca. 10^4 s^{-1} at 298 K, the temperature used in ref 1. Because the intrinsic autodetachment lifetimes of such π^*-anion states of DNA bases are thought[4] to be near 10^{-13} s, we concluded in ref 2 that SSBs induced by this mechanism would occur for only one in 10^9 attached electrons and thus not pose substantial health concerns if the DNA π^*-anions were not further stabilized (e.g., by π-stacking, solvation, or geometric relaxation[5]). However, additional simulations carried out in ref 2, in which the DNA fragment was strongly solvated (using a solvent dielectric constant of 78) showed that the π^*-anion can be rendered stable (i.e., unable to undergo autodetachment), in which case competition between SSB formation and detachment would not take place. Moreover, it was shown that such solvation did not substantially alter the height of the barrier that must be surmounted for C−O bond rupture to occur, so SSB formation was again predicted to occur at a rate of ca. 10^4 s^{-1} but with unit SSB yield per attached electron. In the present work, we extend these solvation studies to include dielectric constants more representative of what the bases, deoxyribose, and neutralized phosphate groups are likely to experience in living organisms.

Before moving on to discuss this work, it is important to again stress that the entire mechanism studied in ref 2 probably would not be operative if the phosphate groups did not have counter-cations (or, in our case, protons) tightly bound to render them neutral. Hence, the findings obtained here, which also involve protonating the phosphate groups to facilitate comparison to the experiments of ref 1, will likely only be relevant to DNA molecules in living systems that, at the time of electron attachment, find the phosphate groups nearest the base to which the electron attaches bound to counterions or other positive charges in close proximity.

In the present paper, we extend our earlier study in several directions:

a. We consider a range of energies (0.2−1.5 eV) for attaching the electron to cytosine's lowest π^*-orbital, which is found in electron transmission experiments to lie ca. 0.5 eV above[4] the neutral cytosine. Exploring such a range of energies is important because the π^*-anion states of DNA's bases are not "sharp" bound states; they are metastable resonance states having finite

lifetimes δt (and hence Heisenberg energy widths δE). We need to explore energies spanning the widths of cytosine's π^*-resonance state to see how the barrier to C−O bond rupture changes as this energy is varied. As discussed above, knowing this barrier is critical to being able to predict SSB formation rates. The special techniques used to describe an electron having kinetic energy in the 0.2−1.5 eV range that attaches to a base π^*-orbital are detailed in the Methods section.

b. We consider a range of solvation environments for the DNA fragment that we use to model the SSB formation process. In ref 2 we considered only nonsolvated and strongly solvated (i.e., $\epsilon = 78$) fragments in order to consider what we believe are likely limiting cases. In the present work, we include other solvation cases including dielectric constants near 4, which likely is more indicative of native DNA. Ultimately, we intend in future work to perform simulations including neighboring (hydrogen bonded and π^*-stacked) bases to more properly model the native environment of such DNA fragments. However, we think it prudent to first examine a range of solvation environments to see how the energy barriers and other findings depend on solvation.

c. We use stabilization-type methods[6] to determine the intrinsic rate at which the attached electron moves from the cytosine's π^*-orbital, through the dexoyribose, and onto the C−O σ^*-orbital. Although the rate-limiting step for forming SSBs turns out to be the rate at which thermal motions cause the C−O bond to access the barrier on the energy surface, it is still important to know how fast the attached electron undergoes this through-bond electron-transfer event. The stabilization method used here allows us to compute the adiabatic rate at which the through-bond electron-transfer process takes place.

II. Methods

Because most of the methods used to carry out these calculations were detailed in ref 2, we will not repeat such a description here. Instead, we will discuss only those methods that are used in this work but that did not appear in our earlier paper.

Because the π^*-anion is not an electronically stable species but is metastable with respect to electron loss, we had to take additional measures to make sure that the energy of the anion relative to that of the neutral fragment shown in Figure 1 was correct. That is, to describe attaching a 1.0 eV electron to the π^*-orbital of cytosine, we needed to alter our atomic orbital basis set to produce a π^*-orbital having an energy of 1.0 eV. We did so by scaling the exponents of the most diffuse π-type basis functions on the atoms within the cytosine ring to generate a lowest π^*-orbital on cytosine with this energy. Of course, we had to perform independent orbital exponent scaling to achieve π^*-orbital energies of 0.2, 0.3, 0.8, 1.0, 1.3, and 1.5 eV (the specific energies studied here). By scaling the atomic orbital basis functions' exponents, we are able to match the kinetic energy of the incident electron to the total (kinetic plus potential) energy of the electron in the cytosine π^*-orbital. This matching is crucial for describing such metastable states.

To describe the effect of surrounding solvent molecules and the π-stacked and hydrogen-bonded bases on the electronic energy and geometry of our model DNA fragment, we employed the polarized continuum (PCM) solvation model[7] within a self-consistent reaction field treatment, and we performed all calculations using the Gaussian 98 program.[8] Dielectric constants of 1.0, 4.9, 10.4, and 78 were included to gain appreciation for how strongly the most important aspects of the resulting data (e.g., barrier heights, through-bond transfer rates) depend on the solvation strength.

The energy profiles that we obtain as functions of the C−O bond length labeled in Figure 1 describe variation in the electronic energy of the cytosine-containing fragment and its anion with all other geometric degrees of freedom "relaxed" to minimize the energy. In duplex DNA, there clearly are constraints placed on the geometry of the cytosine−dexoyribose−phosphate groups (e.g., hydrogen bonding and π-stacking) that do not allow all geometric parameters to freely vary. As such, the energy profiles we obtain provide lower bounds to the barriers that must be overcome to effect C−O bond cleavage. However, we found that the changes in the remaining bond lengths (<0.04 Å) and valence angles (<5°) are quite small as we "stretch" the C−O bond. Hence, we do not think the unconstrained energy profiles result in qualitatively incorrect barriers.

III. Results

A. Energy Profiles. In Figure 3, we show plots of the electronic energies of the neutral and π^*-anion species with various (PCM) solvent dielectric constants for energies of the attached electron ranging from 0.2 to 1.5 eV. The neutral-fragment plots are included to illustrate at what electron energies and solvent conditions the anion is electronically stable and when it is not.

The π^*-anion energy profiles in the absence of solvent (i.e., for $\epsilon = 1.0$) suggest that C−O bond rupture requires surmounting a 8−16 kcal mol^{-1} barrier (depending on the electron energy E) but that the fragmentation process is exothermic in all cases. As discussed earlier, the exothermicity results primarily from the large electron affinity of the neutralized phosphate group $-O-PO_3H_2$ generated by bond rupture. In Table 1, we collect from Figure 3 values of the barrier heights along the C−O bond length for various dielectric constants and various E values, and we show the value of R at which the barrier occurs in each case. Several trends are worth noting:

1. The barrier occurs at nearly the same R-value for all solvents and for all E-values, although there seems to be a trend to smaller R-values at higher E.

2. Among all solvation environments, the barrier ranges from 5 to 28 kcal/mol and is smaller for high E-values than for low E-values. Some of this trend likely derives from the fact that, at higher E, there is more energy present in the anion and thus less energy is needed to access the barrier.

3. Moreover, the barrier tends to grow as the solvation strength increases at low E-values and to decrease as the solvation strength increases at higher E-values.

4. Only for $\epsilon = 1.0$ is the anion electronically metastable; for all other ϵ values, the anion lies below the neutral for all R-values and is thus electronically stable.

B. Predicted Rates of SSB Formation. To estimate the rates of SSB formation, we consider the vibrations of the C−O bond that must rupture. As is typical of most C−O single bonds, this bond is found to vibrate at a rate of ca. 3×10^{13} s^{-1}. The probability P that this C−O bond stretches, through thermal activation at 298 K, enough to surmount a barrier of ΔE is

$$P = \exp(-\Delta E(505)/298)$$

where ΔE is given in kcal mol^{-1} and $505 = 1/R$ with R being the ideal gas constant $R = 1.98 \times 10^{-3}$ kcal (mol K)$^{-1}$. Hence, an estimate[9] of the average rate of SSB formation can be obtained by multiplying the vibrational frequency by the probability of accessing the barrier: $3 \times 10^{13} \exp(-\Delta E(505)/298)$. Using barrier heights ΔE of 5, 10, 15, 20, and 25 kcal mol^{-1}, which characterize the range shown in Table 1, we obtain

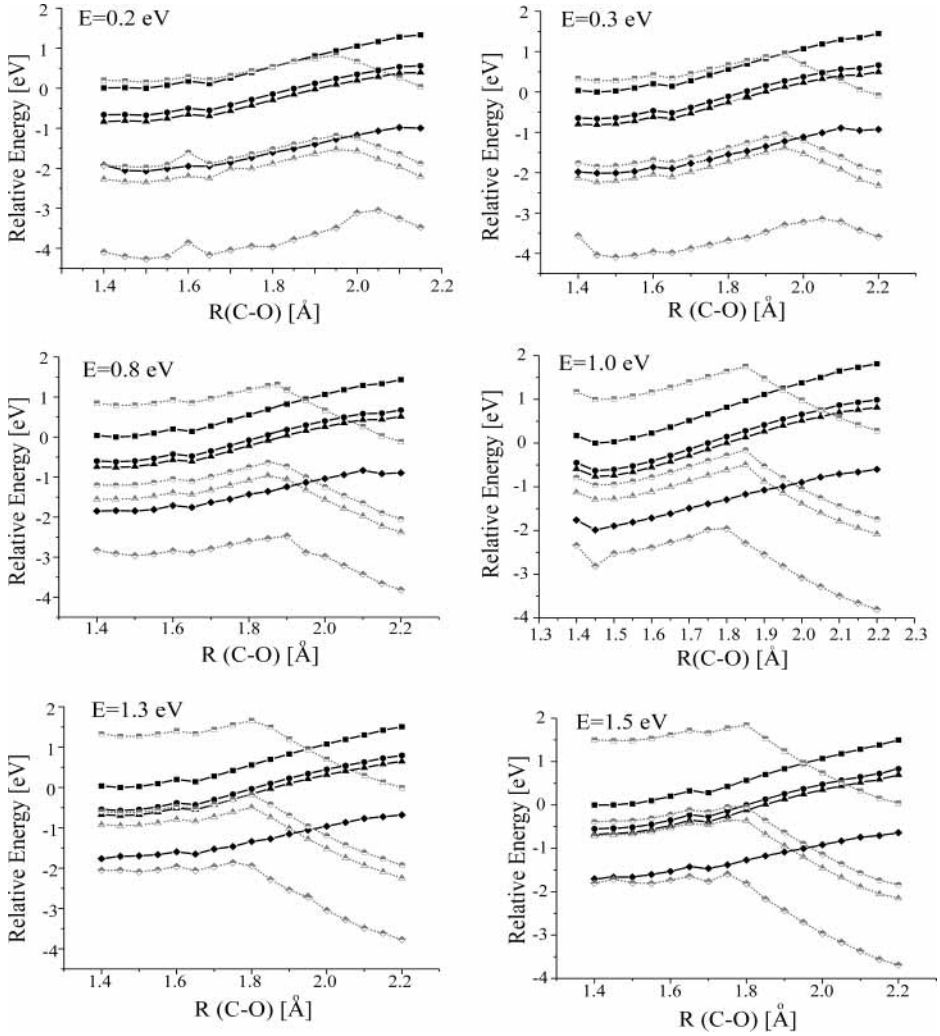

Figure 3. Energies of neutral fragment ($\epsilon = 1.0$, solid square; $\epsilon = 4.9$, solid triangle; $\epsilon = 10.4$, solid circle; $\epsilon = 78$, solid diamond) and of π^*-anion ($\epsilon = 1.0$, half-filled square; $\epsilon = 4.9$, half-filled triangle; $\epsilon = 10.4$, half-filled circle; $\epsilon = 78$, half-filled diamond) fragment at various electron energies E and various solvation dielectric constants.

TABLE 1: Barriers (kcal mol^{-1}) along the C−O Bond Length for Various Electron Kinetic Energies *E* (eV) and Various Solvent Dielectric Constants ϵ as Well as the Value of *R* (Å) Where the Barrier Occurs[a]

electron energy E	0.2	0.3	0.8	1.0	1.3	1.5
barrier ($\epsilon = 1.0$)	15.6	15.1	12.1	11.25	9.0	8.38
barrier ($\epsilon = 4.9$)	18.3	18.5	13.1	10.47	10.2	7.95
barrier ($\epsilon = 10.4$)	19.0	19.8	13.7	10.51	10.5	8.38
barrier ($\epsilon = 78$)	28.1	21.8	11.3	9.5	5.3	5.1
R at barrier ($\epsilon = 1.0$)	1.95	1.95	1.875	1.85	1.80	1.8
R at barrier ($\epsilon = 4.9$)	1.95	1.95	1.85	1.85	1.80	1.8
R at barrier ($\epsilon = 10.4$)	1.95	1.95	1.85	1.8	1.80	1.8
R at barrier ($\epsilon = 78$)	2.05	2.10	1.90	1.8	1.75	1.75

[a] Barrier heights of 5, 10, 15, 20, and 25 kcal mol^{-1} produce C−O rupture rates of 6.3×10^9, 1.3×10^6, 2.7×10^2, 6×10^{-2}, and 1×10^{-5} s^{-1}, respectively.

SSB rates of 6.3×10^9, 1.3×10^6, 2.7×10^2, 6×10^{-2}, and 1×10^{-5} s^{-1}, respectively. As we show in the following section, these rates are slower than the rates at which the attached electron undergoes through-bond electron transfer, and thus it is these rates that we suggest limit the rates of SSB formation whenever the mechanism being examined here is operative.

Recall that the autodetachment lifetimes of π^*-anion states of DNA's bases are expected to be ca. 10^{-13} s when the base is not solvated or has not undergone relaxation to form the electronically stable anion structure. Also, note from Figure 3 that the π^*-anion (of cytosine) is metastable only for $\epsilon = 1.0$. That is, for all the solvent environments considered here, the π^*-anion is electronically stable with respect to the neutral DNA fragment. These observations suggest the following:

a. For nonsolvated DNA (as used in the experiments of ref 1), only at E-values near 1.5 eV will SSB formation be within 3 orders of magnitude of the autodetachment rate. This likely is why the experiments of ref 1 did not observe appreciable SSB formation at energies below ca. 3.5 eV.

b. For moderately or strongly solvated DNA, the anion is electronically stable so competition with autodetachment is not an issue. In such cases, the rates of SSB formation range over many orders of magnitude, but are usually larger at higher E-values and for smaller dielectric constants.

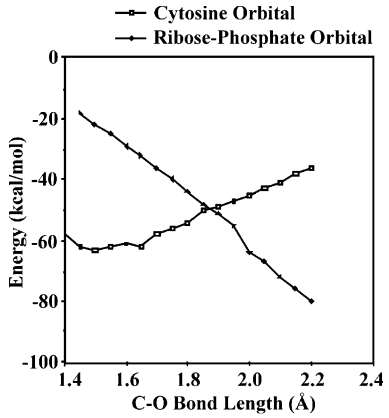

Figure 4. Plots of the π^* (solid line) and σ^* (dashed line) diabatic anion energy states as functions of the C−O bond length *R*.

c. For a dielectric constant near 4, which may be representative of native DNA, the SSB rates range from 10^0 to 10^7 s^{-1} as the electron's kinetic energy varies from 0.2 to 1.5 eV.

C. Rates of Through-Bond Electron Transfer. For each value of the C−O bond length *R* whose variation plays such a crucial role in the SSB formation event, there are two anion states that need to be considered to examine the through-bond electron-transfer event. The first "diabatic" state consists of the DNA fragment with the excess electron attached to cytosine's π^*-orbital at an energy *E* (that can range from 0.2 to 1.5 eV). The second consists of the DNA fragment with the excess electron occupying the σ^*-orbital of the C−O bond. As noted in the Introduction, this latter state lies at much higher energy for *R*-values near R_{eq} (1.45 Å) because it places two electrons into the C−O bonding orbital and one in the C−O antibonding orbital. However, as the C−O bond is stretched, the energy of this σ^*-anion state drops sharply as shown in Figure 4. In fact, the σ^*-anion eventually evolves, at large *R*, into the phosphate anion and a deoxyribose carbon radical. Because the neutralized phosphate group has a large electron binding energy (ca. 5 eV), this σ^*-anion's energy is very low at large *R*. It is this large electron affinity that provides much of the thermodynamic driving force for C−O bond cleavage in the mechanism treated here.

As the C−O bond length approaches 1.9 Å, the σ^*-anion state has decreased enough in energy (because the carbon and oxygen orbitals' overlap has decreased) to render its energy equal to that of the π^*-anion. At such *R*-values, these two diabatic states couple and undergo "avoided crossings" to produce the pairs of adiabatic states whose regions of avoidance are shown in Figure 5 (for various *E*-values).

The energy spacing δE between the two adiabatic curves at their point of closest approach can be used to estimate the rate at which the excess electron, originally localized on the cytosine's π^*-orbital, moves through the unfilled orbitals of the intervening deoxyribose and into the C−O σ^*-orbital. The δE values shown in Figure 5 range from 0.01 to 0.24 eV and correspond to rates of 2×10^{12} to 6×10^{13} s^{-1}. There appears to be no systematic trend in these δE values as the electron energy *E* varies. It is our feeling that this is probably because it is very difficult to identify that precise geometry at which the π^*-and σ^*-anion states have their minimum splitting (it is this energy gap that defines δE). As a result, we experience considerable numerical uncertainty in the δE values that we report, but the resultant predicted transfer rate range of 10^{12}−10^{14} s^{-1} likely is valid.

Recall that in Figure 2 we showed the singly occupied molecular orbital[10] of our anion fragment near the equilibrium value of *R*, where the electron occupies the cytosine π^*-orbital, and at large *R*, where the electron resides between the phosphate and sugar groups. It is the rate of this through-bond electron-transfer event that the energy spacings shown in Figure 5 allow us to estimate. The above plots and Figure 2 clearly show that the attached electron can indeed migrate "smoothly" from the π^*-orbital of cytosine and onto the phosphate. We again note that the deduced through-bond electron-transfer rates are much faster than the rates at which the barriers shown in Figure 3 are accessed. For this reason, the overall rate of electron migration and of SSB formation will be determined by the rate at which the barriers on the surface are surmounted, not by the through-bond transfer rate.

IV. Summary

Our ab initio simulations have been aimed at studying the rates at which very specific single strand breaks occur in DNA after a free electron attaching to a base within the DNA. The particular mechanism studied here likely will be operative only when the negatively charged phosphate groups closest to the base to which the electron attaches have nearby countercations or some other positive charges that render them neutral. This was, of course, the case for the DNA molecules used in the original experiments[1] that attracted our interest in this phenomenon. Only in such situations will the electron transfer from the base's π^*-orbital to the phosphate group be energetically as favorable as in this case.

We view the sequence of events taking place in this mechanism as follows.

1. An electron having kinetic energy *E* in the range 0.2−1.5 eV (as studied here) attaches to the lowest π^*-orbital of cytosine. This state has a maximum in its attachment cross section[4] near 0.5 eV but extends considerably above and below this energy; this is why we compute rates for *E* values between 0.2 and 1.5 eV for this single resonance state. The incident electron cannot enter the C−O σ^*-orbital directly because this orbital's energy is too high when the C−O bond is near its equilibrium distance.

2. In the absence of stabilization due to surrounding hydrogen-bonded or π-stacked bases or solvent molecules or even vibrational relaxation, the π^*-anion state can undergo electron autodetachment at a rate of ca. 10^{13} s^{-1}.

3. Alternatively, after attachment, the π^*-anion may undergo geometric distortion and/or reorganization of the surrounding solvation environment to render this state electronically stable. We find that even modest solvation makes the π^*-anion stable, so it is likely that a significant fraction of the nascent π^*-anions become stabilized.

4. As the π^*-anion's C−O bond vibrates (with frequency ν) under thermal excitation, it has some (albeit low) probability of reaching a critical distortion at which the C−O bond's σ^*-orbital and the base's π^*-state become nearly degenerate. The energy ΔE required to access such a stretched C−O bond plays a crucial role in determining the rate (given as $\nu \exp(-\Delta E/RT)$) of C−O bond cleavage and thus of SSB formation. We find these barriers ΔE to vary from ca. 5 to 28 kcal mol^{-1}; they are smallest at higher *E*-values and they depend on the solvation environment as shown in Table 1. The energies ΔE are, in effect, the reorganization (including solvent and intramolecular relaxation) energy requirements for the electron-transfer event to occur.

5. Once the barrier is reached at the stretched C−O bond length, the attached electron promptly moves, via a through-bond transfer process, from the base's π^*-orbital, through the

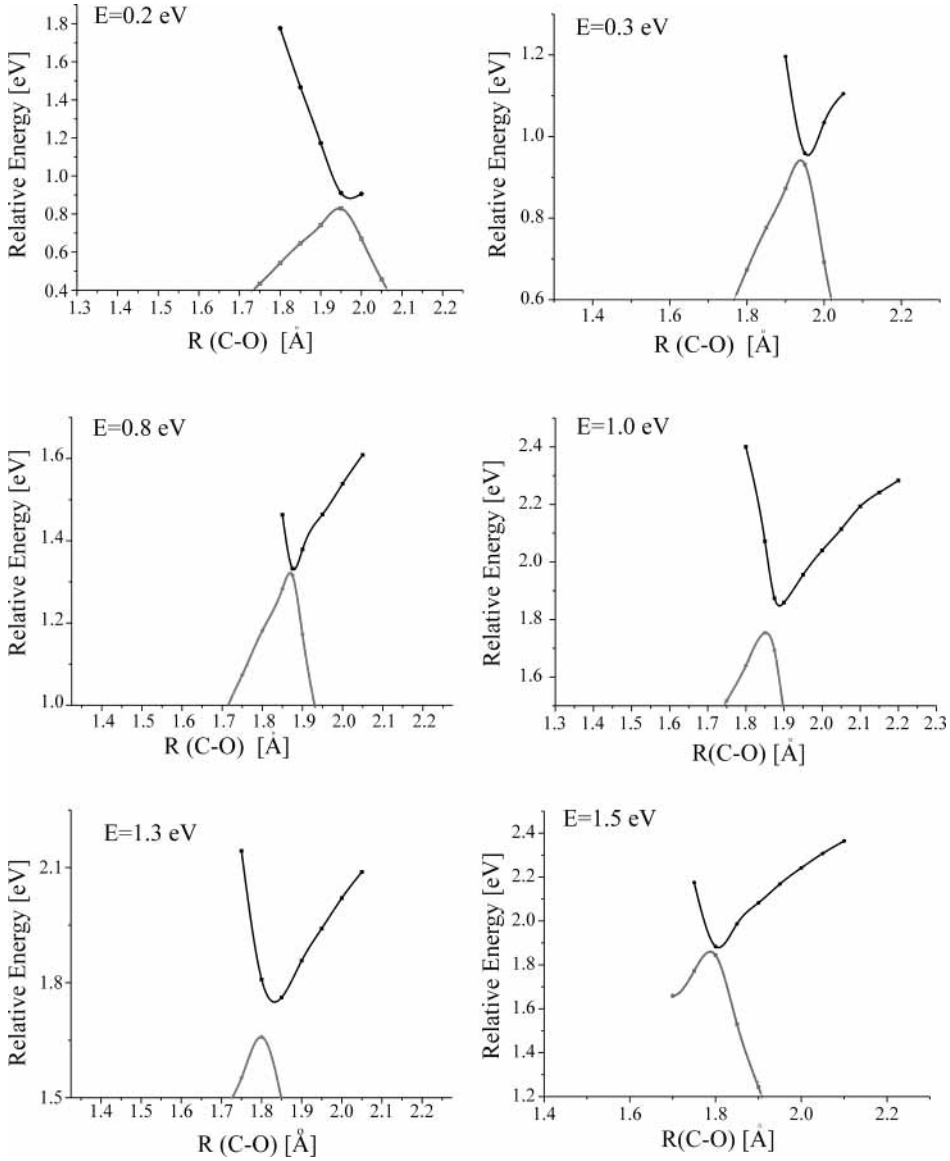

Figure 5. Avoided crossings between π^*- and σ^*-anion states for nonsolvated DNA fragment at various *E*-values. The pairs of curves represent the adiabatic energies of the two anion states.

vacant orbitals of the intervening dexoyribose, and onto the C−O bond that eventually cleaves to produce the highly stable phosphate ion. We find that the rate of through-bond electron transfer is faster than the rate of accessing the barrier, so the former is not the rate-limiting step in forming SSBs.

It should be recalled that the samples used in the experiments of ref 1 contained dried DNA, so the degree of solvation in those experiments was quite low. For this reason, the anions formed by electron attachment in those experiments were probably electronically metastable with lifetimes in the 10^{-13} s range, as a result of which the yield of SSBs per attached electron was quite low (in fact, SSBs were not even observed at the low *E*-values considered here although they were at *E*-values above 3.5 eV). However, because even modest solvation is shown here to render the π^*-anion state electronically stable, the yields of SSBs per attached electron can approach unity if the phosphate groups near the base to which the electron attaches are rendered neutral by countercations or other positive charges. Certainly, such is not the case for the vast majority of DNA molecules in living species, but it may occur often enough (e.g., as cations migrate into the neighborhoods of the phosphate groups) to make the mechanism suggested here and in ref 2 important to be aware of.

Acknowledgment. This work was supported by NSF Grants 9982420 and 0240387 to J.S. and Grant DS/8371-4-0137-3 to P.S. The computer time provided by the Center for High Performance Computing at the University of Utah is also gratefully acknowledged.

References and Notes

(1) Boudaiffa, B.; Cloutier, P.; Hunting, D.; Huels, M. A.; Sanche, L. *Science* **2000**, *287* (5458), 1658−1662.

(2) Barrios, R.; Skurski, P.; Simons, J. *J. Phys. Chem. B* **2002**, *106*, 7991.

(3) Stubbe, J.; Kozarich, J. W. *Chem. Rev.* **1987**, *87*, 1107. Giloni, L.; Takeshita, M.; Johnson, F.; Iden, C.; Grollman, A. P. *J. Biol. Chem.* **1984**, *236*, 8608. Burrows, C. J.; Muller, J. C. *Chem. Rev.* **1998**, *98*, 1109−1151.

(4) It had been shown in the following reference that low-energy electrons indeed can be captured into the low-lying π^*-orbitals of DNA's bases: Aflatooni, K.; Gallup, G. A.; Burrow, P. D. *J Phys. Chem. A* **1998**, *102*, 6205−6207. Moreover, in ref 1, it was speculated that the initial electron capture event involved the base π^*-orbitals.

(5) Desfancois, C.; Periquet, V.; Bouteiller, Y.; Schermann, J. P. *J. Phys. Chem. A* **1998**, *102*, 1274−1278. Al-Jihad, I.; Smets, J.; Adamowicz, L. *J. Phys. Chem. A* **2000**, *104*, 2994−2998. In these papers, it is shown that the bases can have positive adiabatic yet negative vertical electron affinities. In the electron capture process, the vertical value applies, but subsequent vibrational relaxation can allow the base anion to become electronically stable.

(6) (a) Hazi, A. U.; Taylor, H. S. *Phys. Rev. A* **1970**, *1*, 1109−1116. (b) Whitehead, A.; Barrios, R.; Simons, J. *J. Chem. Phys.* **2002**, *116*, 2848−2851. (c) Bacic, Z.; Simons, J. *J. Phys. Chem.* **1982**, *86*, 1192−1200. (d) Simons, J. *J. Chem. Phys.* **1981**, *75*, 2465−2467.

(7) Miertus, S.; Scrocco, E.; Tomasi, J. *Chem. Phys.* **1992**, *55*, 117. Miertus, S.; Tomasi, J. *Chem. Phys.* **1982**, *65*, 239. Cossi, M.; Barone, V.; Cammi, R.; Tomasi, J. *Chem. Phys. Lett.* **1996**, *255*, 327.

(8) Frisch, M. J.; Trucks, G. W.; Schlegel, H. B.; Scuseria, G. E.; Robb, M. A.; Cheeseman, J. R.; Zakrzewski, V. G.; Montgomery, J. A., Jr.; Stratmann, R. E.; Burant, J. C.; Dapprich, S.; Millam, J. M.; Daniels, A. D.; Kudin, K. N.; Strain, M. C.; Farkas, O.; Tomasi, J.; Barone, V.; Cossi, M.; Cammi, R.; Mennucci, B.; Pomelli, C.; Adamo, C.; Clifford, S.; Ochterski, J.; Petersson, G. A.; Ayala, P. Y.; Cui, Q.; Morokuma, K.; Malick, D. K.; Rabuck, A. D.; Raghavachari, K.; Foresman, J. B.; Cioslowski, J.; Ortiz, J. V.; Baboul, A. G.; Stefanov, B. B.; Liu, G.; Liashenko, A.; Piskorz, P.; Komaromi, I.; Gomperts, R.; Martin, R. L.; Fox, D. J.; Keith, T.; Al-Laham, M. A.; Peng, C. Y.; Nanayakkara, A.; Gonzalez, C.; Challacombe, M.; Gill, P. M. W.; Johnson, B. G.; Chen, W.; Wong, M. W.; Andres, J. L.; Gonzalez, C.; Head-Gordon, M.; Replogle, E. S.; Pople, J. A. *Gaussian 98*, Revision A.7; Gaussian, Inc.: Pittsburgh, PA, 1998.

(9) Alternatively, one can employ a transition-state approximation to compute the rate of barrier crossings. Doing so (using harmonic vibrational frequencies) produces (at 298 K) a rate given by $7 \times 10^{13} \exp(-\Delta E(505)/298)$. Clearly, using the partition functions within the transition-state framework more properly accounts for entropic changes, but does not qualitatively alter the estimates. Hence, we have chosen to make our SSB formation rate estimates using the simple model outlined earlier.

(10) These plots were obtained using the MOLDEN program: Schaftenaar, G.; Noordik, J. H. MOLDEN: a pre- and post-processing program for molecular and electronic structures. *J. Comput.-Aided Mol. Des.* **2000**, *14*, 123.